Thermal analysis of HeII cooled Nb3Sn coil samples for High Luminosity upgrade of the LHC

Kirtana Puthran

kirtana.puthran@cern.ch

TE-MSC-SCD, CERN

Rob van Weelderen

rob.van.weelderen@cern.ch

Carried out during junior fellowship at
Central Cryogenics Laboratory,
Cryogenics Research Group
TE-CRG-CI, CERN

Goals

There exist several open questions with respect to cooling and mechanical integrity of the Nb3Sn magnets.

In context of thermal behaviour, an test program has been ongoing at the Cryolab, involving experimentation and numerical simulation of the 11T dipole (D11T) and inner triplet quadrupoles (MQXF) for HiLumi LHC.

1. **Experimental campaign** to measure thermal behavior of D11T and MQXF samples.
   - From prototype to present series production coil samples.
     S/O Lise E. Murberg, Torsten Koettig
2. Evolution of a robust multi-region end to end **numerical toolkit**.
   - Solvers for static HeII and solids with varying thermal properties.
   - Boundary conditions for thin-resistive layers, and interface resistances.
   - Capability of easy parameterisation studies to predict and optimise operational requirements.

Introduction

Heat deposition in D11T magnet coil pack (Latest lattice position)

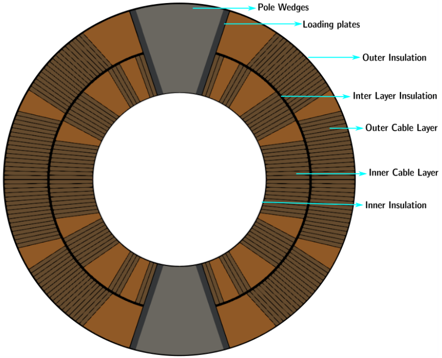

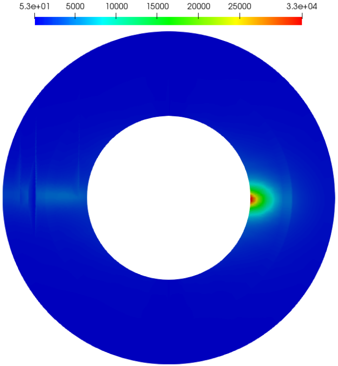

Coil Layer	Peak Power Dep. $\mathrm{mW/cm^3}$
Inner	32.9237
Outer	3.8166

- Particle losses from beams
- Interaction between particles
- Collisions with m/s dust particles, etc.

2760 bunches with 2.3E11 protons/bunch, 8.81E11 protons/s loss rate

Courtesy: Andreas Waets, Anton Lenchner; SY/STI/CERN

Experiment

Representative Sample, Heating Methods

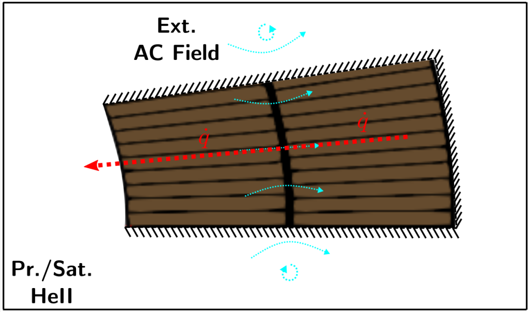

AC heat loss generation, internal/joule heating

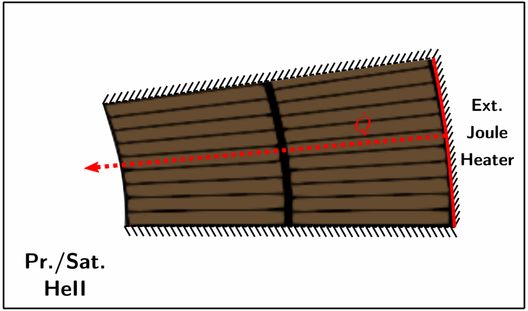

External heating

- AC heat loss mechanisms driven by an external SC NbTi coil to induce homogeneous heat generation, $\dot{q}[W/m^3]$ internally within the cables.
- Calibration of heat inputs to sample with a heat meter.

- Resistive kapton heater of 65 Ω placed on outer surface of sample before insulation, creating constant heat flux, $\dot{Q}[W/m^2]$ through sample cross-section.
- Sample is insulated such that that 99.3% heat will go into the sample.

Experiment
Sample Preparation

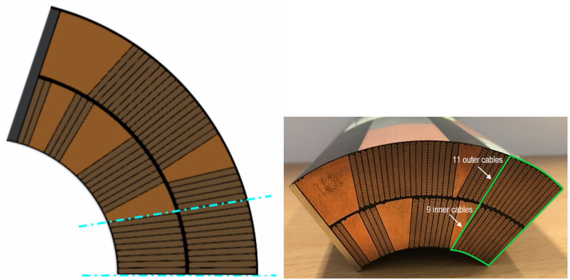

Quarter section from Coil GE02 as obtained. Section cut out as sample marked.

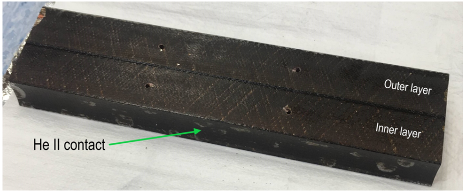

Cut sample (D11TGE02) with sensor holes drilled, **two in each cable layer**. Inner surface exposed to He II is shown.

- Section of the coil predicted to experience the peak heat loads is chosen for cutting out the sample, about 140 mm in length, determined by setup[1]capacity.
- Four holes of typically 1.4 mm diameter for each of the temperature sensors (Cernox^{TM} bare-chip) are carefully drilled into the cable layers at equal lengths from the ends such that the sensors can be placed in the center of the cable layer cross section.

[1] Description in Appendix

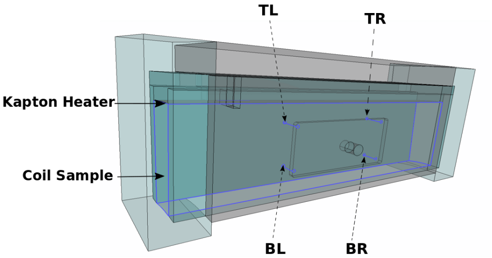

Tests in	Sample Name	Coil Trace
2017	D11T Proto	In-House
2020	D11T GE02	Coil GE02
2018, 19, 20	MQXF LARP07	LARP
2021	MQXF P06	Coil P06, MQXFAP1b

Samples insulated to allow only inner surface in direct contact with He II.

- Prototype samples tested only with AC heat loss gen. method.
- Production samples include resistive kapton heater of 65 Ω placed on outer surface of bare sample.

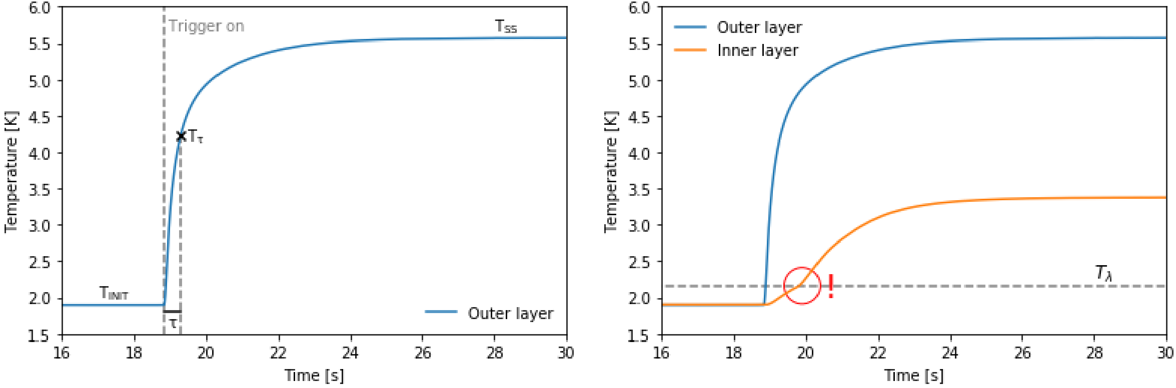

Typical measurement for each heat input, at a given bath temperature

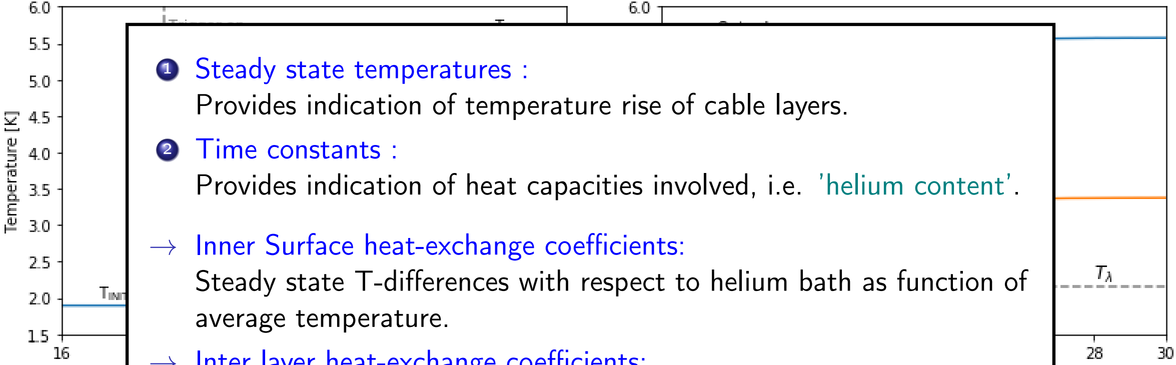

1. Steady state temperatures :
   Provides indication of temperature rise of cable layers.
2. Time constants :
   Provides indication of heat capacities involved, i.e. 'helium content'.

→ Inner Surface heat-exchange coefficients:
Steady state T-differences with respect to helium bath as function of average temperature.

→ Inter layer heat-exchange coefficients:
Steady state T-differences between the coil layers allows for insulation material data comparison.

→ Kapitza Conductance

Experiment Results

Steady State Behaviour - Production Samples

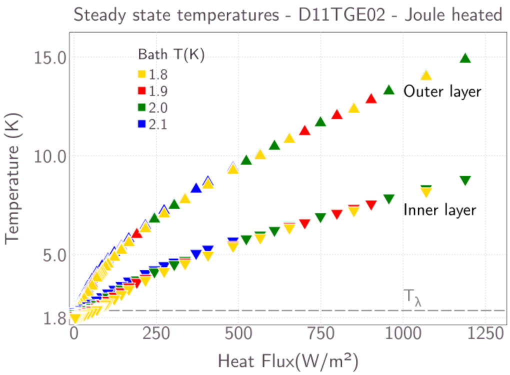

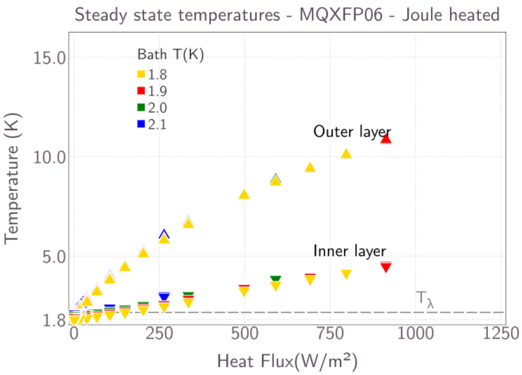

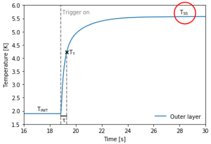

- At low heat loads $\approx 250 \mathrm{W/m^2}$, effect of bath temperature pronounced.
- At high heat loads, ΔT temperature irrespective of bath temperature (see extracted transfer coeffs., slide)
- Difference in curvature for inner cable layer at low[2]and high heat load, an indication of effect of helium, elaborated in data analysis slides.

[2] See Appendix

Experiment Results
Transient Behaviour - Production Samples

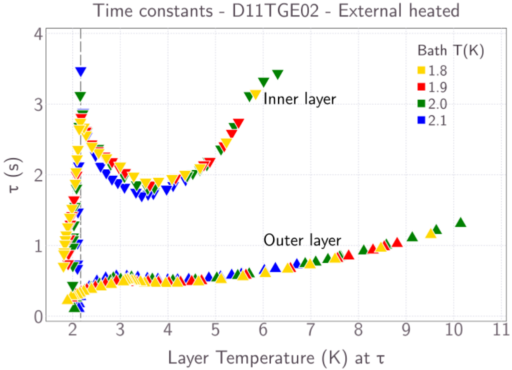

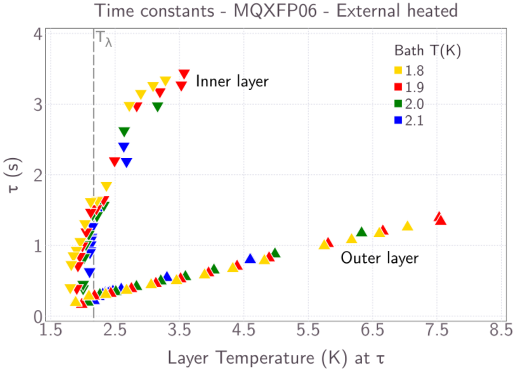

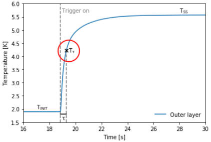

- For GE02, inner layer peak at T_λ with time constants up to 3.44 s, indicating He II presence, No indication of He II presence in outer layer.
- For P06, no indication of He II presence in both layers.
- Indication of He II presence in both layers for prototype samples[3].

[3] See Appendix

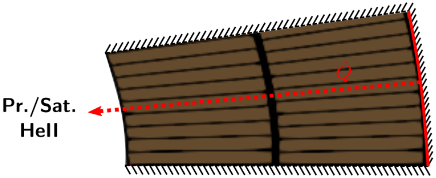

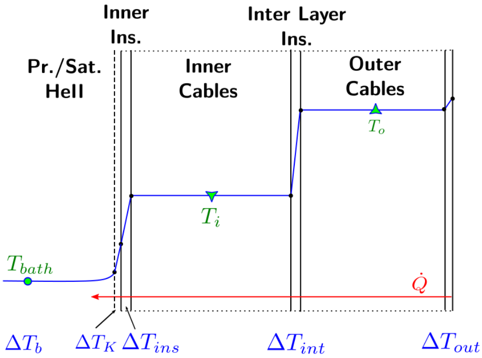

- Transfer coefficient at inter layer insulation :

$$h_{int} = \frac{(T_o - T_i)}{\dot{Q}} \qquad (1)$$

- Total transfer coefficient at inner surface :

$$h_{inn} = \frac{(T_i - T_b)}{\dot{Q}} \qquad (2)$$

Data Analysis - 1

Transfer coefficients at inter layer insulation

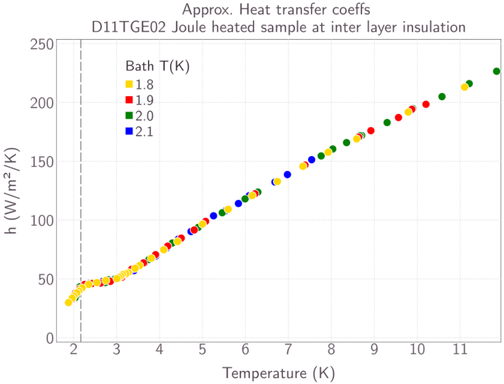

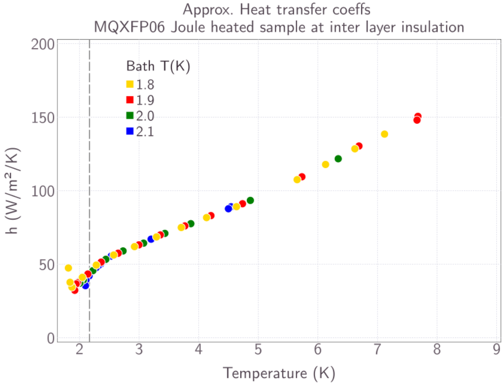

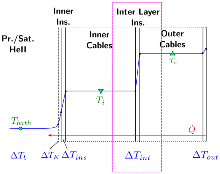

- At (average) temperatures higher than $\sim 3\,\text{K}$, convergence in transfer coefficients irrespective bath temperature.

Data Analysis - 2

Approx. conductivity of inter layer insulation

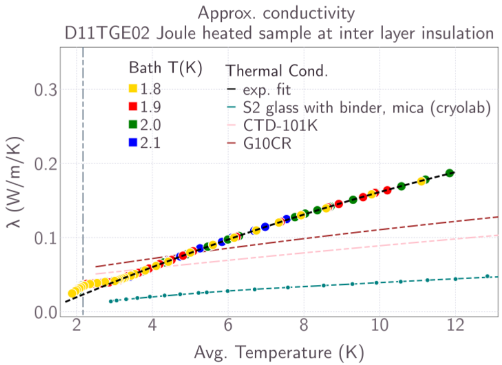

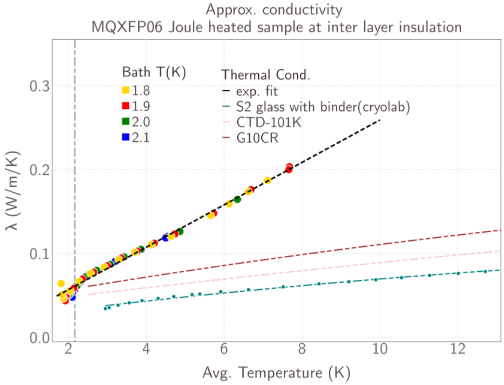

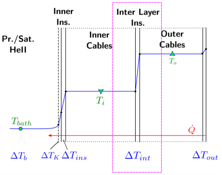

- Deviation from material data.
- Difference in inter-layer insulation conductivity between samples.

→ Possible factors? Type/components of glass fibre, VPI, curing , compression load...

Data Analysis - 3

Transfer coefficients at inner insulation

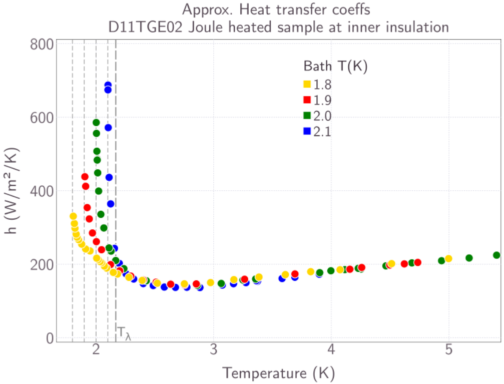

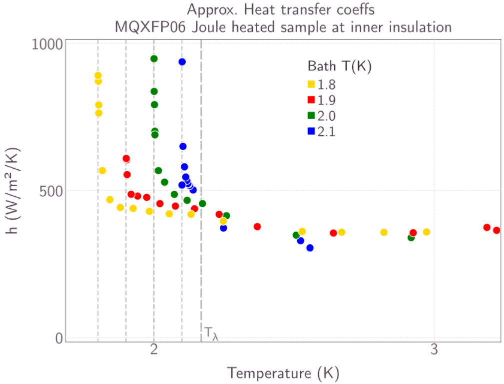

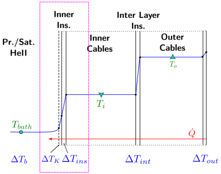

- Below 3 K, effect of Kapitza conductance or helium presence either within the inner insulation is predominant, or both.
- At average temperatures higher than 3 K, convergence in transfer coefficient.
- D11T sample shows lower transfer coefficient than MQXF sample (about factor 2), contrary to as expected from only a dimensional difference.

Data Analysis - 4

Kapitza Resistance Fits

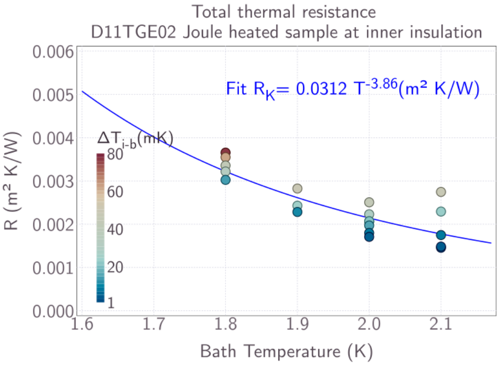

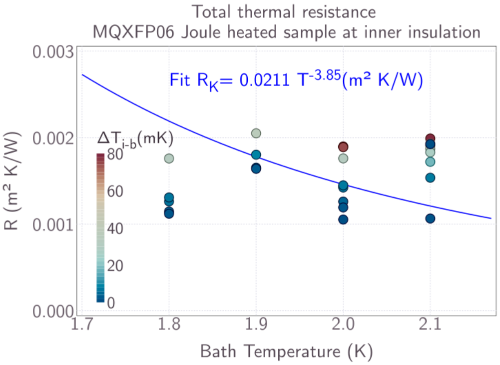

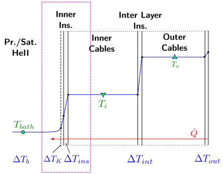

- At very low fluxes, ΔT_K dominates the contribution to ΔT_{inn}.
- Assuming fairly constant resistance, $R_K = A\frac{\Delta T_K}{\dot{Q}}$ for $\Delta T_K < 80\,mK$, kapitza transfer coefficient at inner surface can be estimated, using power fits ($\mathrm{AT^{-n}}$).
-

Data Analysis - 4

Kapitza resistance Fits

- → Resistance fits are over estimated for samples, since surface temp. is not truly known.
- → But, cannot be ignored for a good simulation.

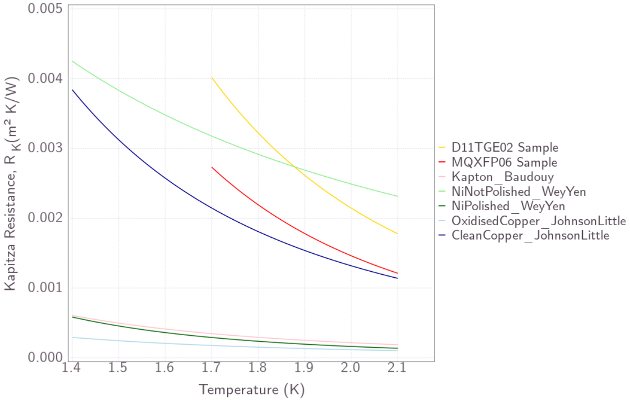

Numerical Analysis

Components

- Geometry, Mesh
- Solver $\rightarrow$ Conjugate heat transfer; Static HeII, Solid
- Special boundary conditions
- Low temperature material properties
- Convergence criteria
- Simulation time $\rightarrow$ Parallel computing
- Helium content in solid regions
- Validation of model
- Extrapolation to full magnet cross-sections to simulate peak power deposition scenarios.

Open-source..

1. 1D Heat Transfer Model [Julia]
    - 4 region composite solid with semi implicit solver.
    - Phenomological model for estimation of helium content.
    - Intensive parameter studies for dimensional and material property variation.
2. 2D, 3D Heat Transfer Model [Salome, OpenFoam(C++ toolbox)]
    - Modular.
    - 1 composite region instead of several.
    - Separate libraries for helium properties and solids.
    - Includes model for implementing helium content.

1. For steady state heat transport, from two-fluid model, if no net mass flow;

$$\nabla T = -\frac{\beta \mu_n q}{d^2 (\rho s)^2 T} - f(T,p) q^m \quad (3)$$

where,

$$K_L = -\frac{d^2 (\rho s)^2 T}{\beta \mu_n} \quad (4)$$

$$K_{eff-GM} = \left(\frac{f^{-1}(T,p)}{|\nabla T|^2} \right)^{\frac{1}{m}} \quad (5)$$

Sato's correlation[4], with m = 3.4:

$$f^{-1}(T,p) = h(t) g_{peak}(p) \quad (6)$$

Energy equation :

$$\rho C_p(p,T) \frac{\partial T}{\partial t} = \nabla \cdot K_{eff} \nabla T \quad (7)$$

? For wide channels, normal fluid viscous term is neglected, but initial singularity due to $|\nabla T|$!

× Introducing small initial gradient leads to numerical errors.

◇ Search for a critical gradient by equating laminar and turbulent regimes' gradient, but β and d for laminar regime is defined for specific geometries, plus in reality, a transition regime exists.

- For solid regions, standard heat conduction equation ;

$$\rho C_p(T)\frac{\partial T}{\partial t} = \nabla \cdot (k(T)\nabla T) + \dot{q} \tag{8}$$

Possibilities:

- HeII in porous media (Macroscopic model)
  $\rightarrow$ Pore size or porosity, permeability, specific surface area, tortuosity

- Conjugate heat transfer (Microsopic model)
  $\rightarrow$ Statistical distribution of shape and size, Kapitza, computationally v intensive.

- Phenomenological model for composite system
  $\rightarrow$ Surface/Volume Fraction of HeII

  1. Thermal conductivity[5](Semi-empirical model needed)

$$k = (1 - \phi_s)k_{solid} + \phi_s k_{HeII} \tag{9}$$

  uses eqns. 4 & 5 for k_{HeII}

  2. Heat capacity

$$\rho C_p = (1 - \phi_v)(\rho C_p)_{solid} + \phi_v(\rho C_p)_{HeII} \tag{10}$$

[5] Progelhof, R. C., J. L. Throne, and R. R. Ruetsch. "Methods for predicting the thermal conductivity of composite systems: a review." Polymer Engineering & Science 16.9 (1976): 615-625.

Simulation - 1D

D11TGE02 sample at 1.9 K

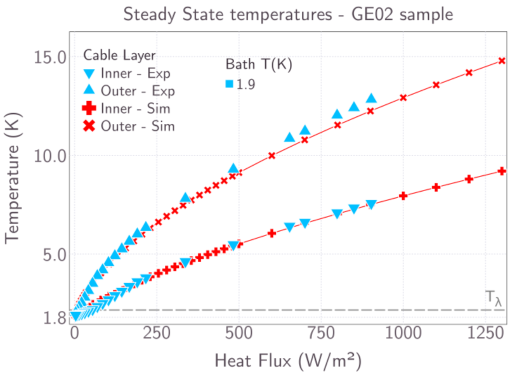

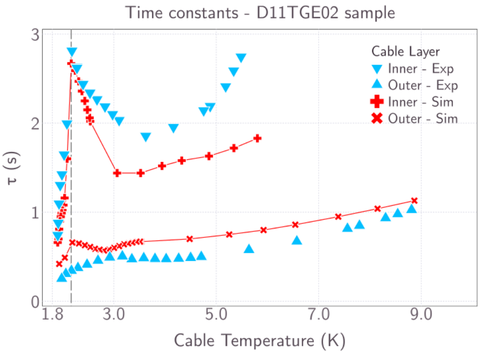

- Using extracted Kapitza resistance fit and extracted interlayer conductivity, steady states are fairly acceptable.
- Volume-fraction based helium content to estimate possible non-homogeneous helium content, however very sensitive.
- 0.32% estimated helium content in inner cable layer, by volume fraction.

Simulation - 1D

Comparing prototype & production samples

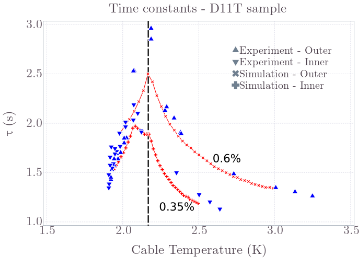

Prototype, only ϕ_v

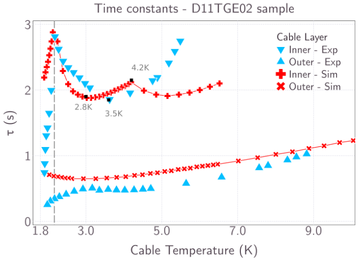

Production, only ϕ_v

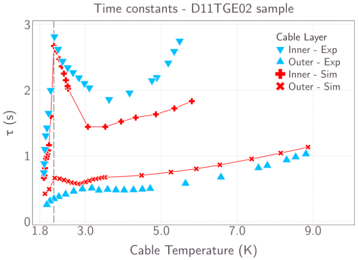

Production , both ϕ_s , ϕ_v

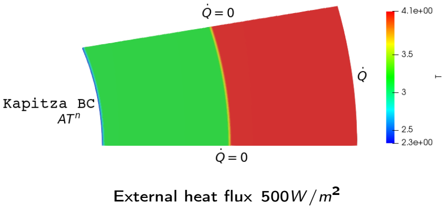

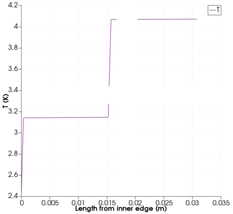

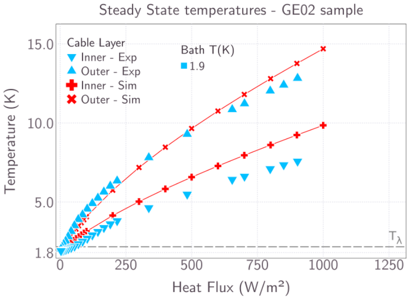

- Using measured coil sample characteristics, conservative estimates of max. temperature are made.
- 2D Model overestimates the inner cable layer values, since data extraction under 1D assumption.

Simulation 2D

11T Full Coil at Peak Power Load : Temperature Map

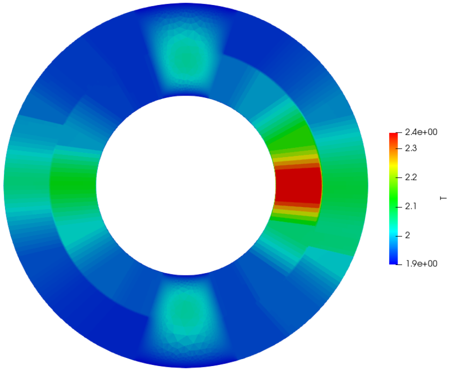

Nominal peak power $\approx 32 mW/cm^3$,
heat map in slide 3

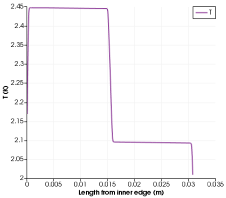

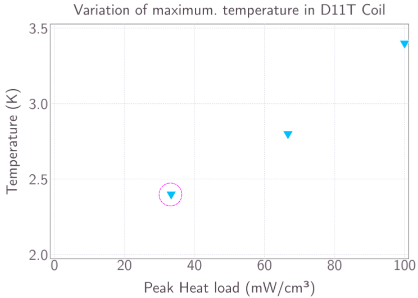

with factored heat maps

- Using measured coil sample characteristics, conservative estimates of max. temperature are made.
- Maximum coil temperature estimation for up to 3 times predicted peak load ($\approx 100\mathrm{mW}/\mathrm{cm}^3$) remains within the temperature range of 1.9 K - 3.5 K, i.e below T_{margin} .

Summary

- External heating method is preferred method for further samples.
- 1D heat transfer model maybe used for fast and vast parametric studies, but has limitations for extension.
- OF model validated with experiments on coil samples (with estimated material props.) and extrapolated for coil pack. Models could be upgraded as more experimental data is generated.
- Upgraded version is far simpler to use, and computation power needed is much less. Phase 2 versions will be benchmarked on the cluster.

Summary

✓ Production samples showed less or no helium content in the cable layers compared to prototype samples. Analysis of thermal transients show improvement from 0.35% inner layer and 0.6% outer layer of prototype coils to 0.32% inner and ∼0% outer layer in production coils, by volume fraction.

? Literature data is incomplete or missing for thermal conductivity and heat capacity, of coil materials and their (old and new) dielectric insulation materials.

? HeII penetration due to porosities might be contributing factor to cable degradation → ongoing cyclic heat load experiments at cryolab.

Thank you!

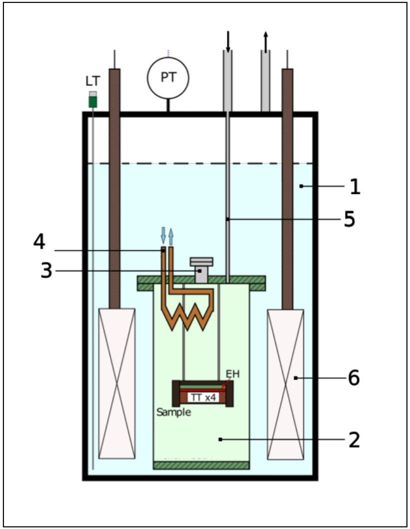

Aims to replicate the conditions as seen by the magnet coils in operating conditions, with two sample heating methods

- Vertical cryostat, with two separated volumes of liquid helium.
  - ↠ Outer saturated bath [1]
  - ↠ Inner pressurised bath (with sample), in G11 pot [2]
- Burst Disc [3]
- Temperature control via. Cu heat exchanger [4]
- Pressurisation control [5]
- External NbTi Magnet, for AC loss gen. method [6]

Data Analysis

Transfer coefficients (global) at inner surface - GE02 - External vs. Inductive heating

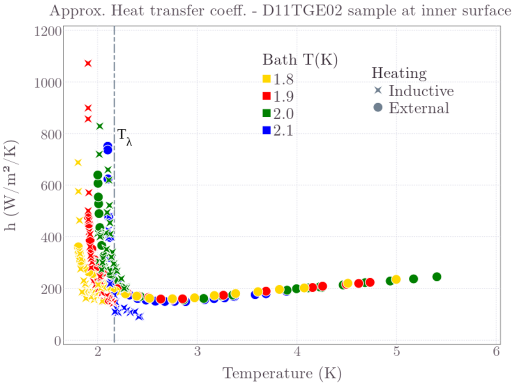

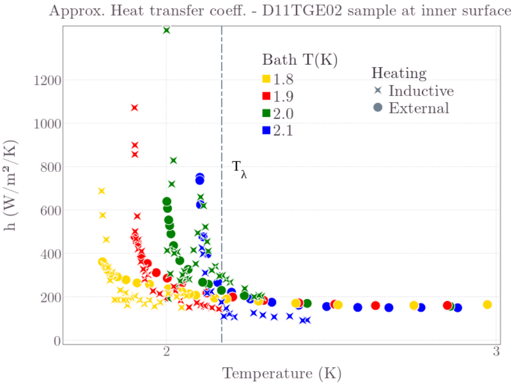

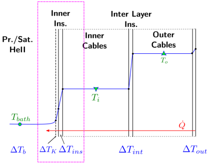

- Above T_λ, tendency towards slightly lower transfer coefficients obtained with joule heating (could be attributed to difference in heating method, to be quantified).
- Below T_λ, coincidence of coefficients between heating methods is seen.

Data Analysis

Transfer coefficients (global) at inner surface - D11T production vs. prototype sample

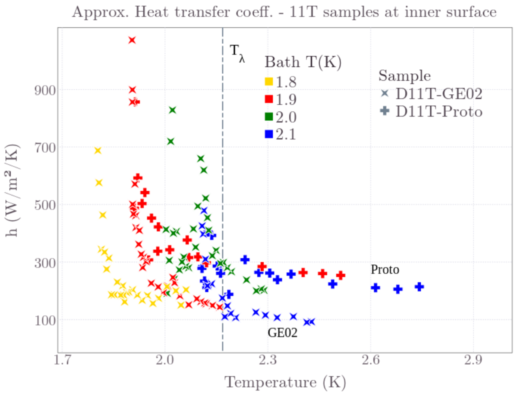

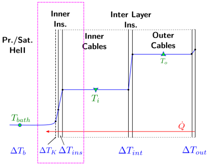

- Lower transfer coefficients obtained with new sample, suggesting effect of lower helium content.

Experiment Results

Steady State Behaviour

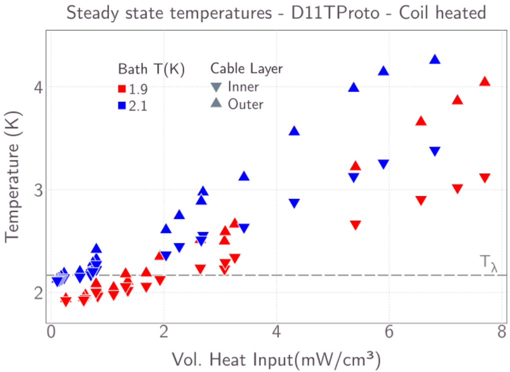

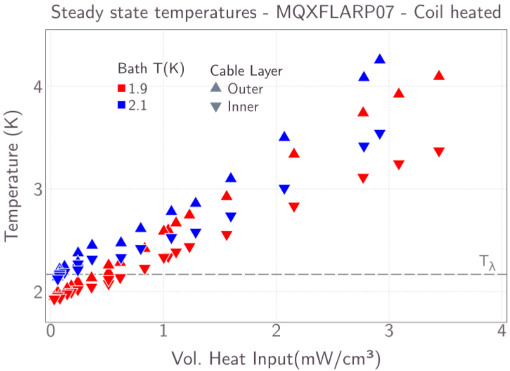

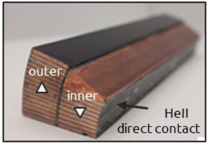

- Cable temperatures reaching upto 4 K, with outer layer reaching higher temperatures due to longer thermal path.
- Steady States cross T_λ.
- MQXF-sample shows less efficient heat exchange than 11T-sample.

Experiment Results
Transient Behaviour

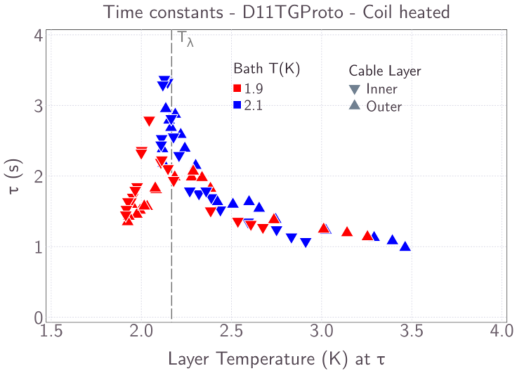

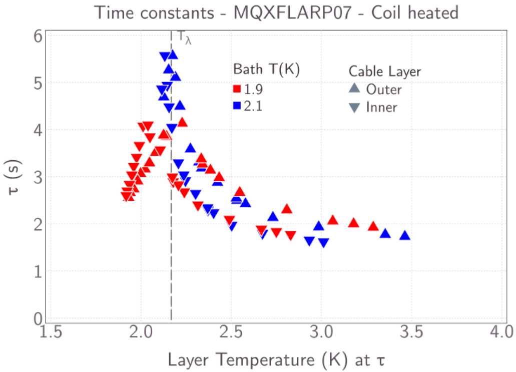

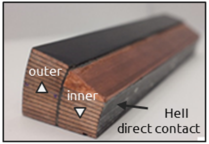

- Evident signature of helium presence due to λ-peak shape (i.e. c_p of helium).
- MQXF sample time constants 2x that of D11T.

Simulation
Proto Samples

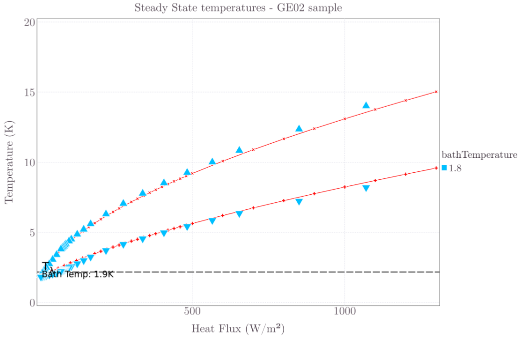

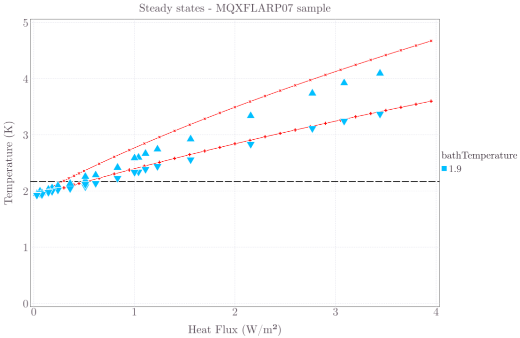

- 1D implicit heat transfer numerical model, with transfer coefficient for convection boundary condition at He interface from experiment data estimation.
- Simulated steady state temperatures follow closely to experiments.

Simulation - 1D

Proto Samples

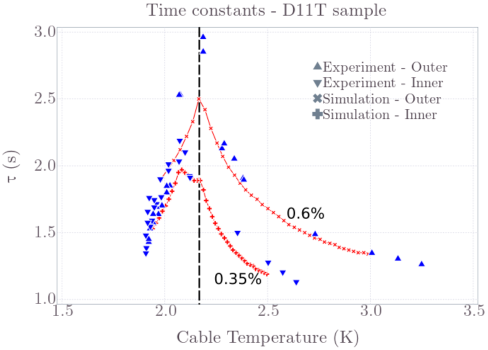

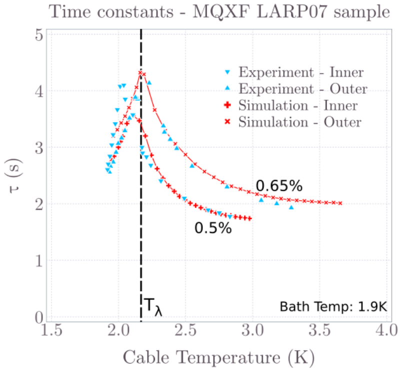

- Volume-fraction based heat capacity to estimate non-homogenous helium content.
- For D11T sample, estimated distribution of 0.35 % and 0.6 % He in inner and outer layer, respectively.
- For MQXF sample, distribution of 0.4 % He and 0.65 % He is estimated in inner and outer layer, respectively.

Magnet Geometries

Drawing Cross-Sections

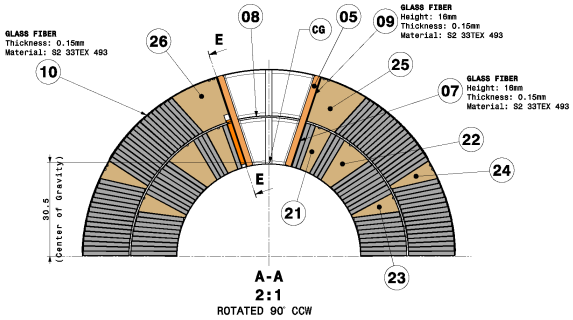

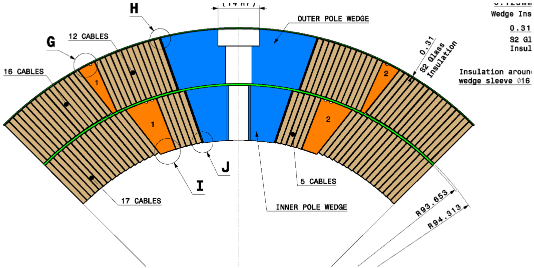

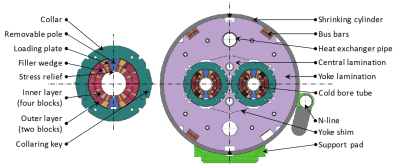

D11T

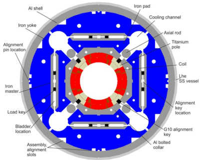

MQXF

[6]Considering a symmetry of normal $\leftrightarrow$ superfluid mass transfer (to avoid defining an ill-posed problem), the momentum equations for the normal and superfluid components are respectively;

$$\frac{\partial \rho_n \mathbf{v}_n}{\partial t} + \nabla \cdot (\rho_n \mathbf{v}_n \mathbf{v}_n) = -\frac{\rho_n}{\rho} \nabla p - \rho_s s \nabla T + \nabla \cdot (\mu_n \nabla \mathbf{v}_n) - A \rho_n \rho_s |\mathbf{v}_n - \mathbf{v}_s|^2 (\mathbf{v}_n - \mathbf{v}_s) + [r_{ns} \mathbf{v}_s - r_{sn} \mathbf{v}_n] \quad (11)$$

$$\frac{\partial \rho_s \mathbf{v}_s}{\partial t} + \nabla \cdot (\rho_s \mathbf{v}_s \mathbf{v}_s) = -\frac{\rho_s}{\rho} \nabla p + \rho_s s \nabla T + A \rho_n \rho_s |\mathbf{v}_n - \mathbf{v}_s|^2 (\mathbf{v}_n - \mathbf{v}_s) - [r_{ns} \mathbf{v}_s - r_{sn} \mathbf{v}_n] \quad (12)$$

$\rho_s s \nabla T$ term represents the thermomechanical force which occurs due to a temperature gradient, responsible for creating counterflow of the components. Energy Conservation Equation, which is determined only by normal fluid is;

$$\frac{\partial \rho s}{\partial t} + \nabla \cdot (\rho s \mathbf{v}_n) = \nabla \cdot (\frac{k_n}{T} \nabla T) + \frac{A \rho_n \rho_s |\mathbf{v}_n - \mathbf{v}_s|^4}{T} \quad (13)$$

[6]Helium Cryogenics, Steven. W. Van Sciver